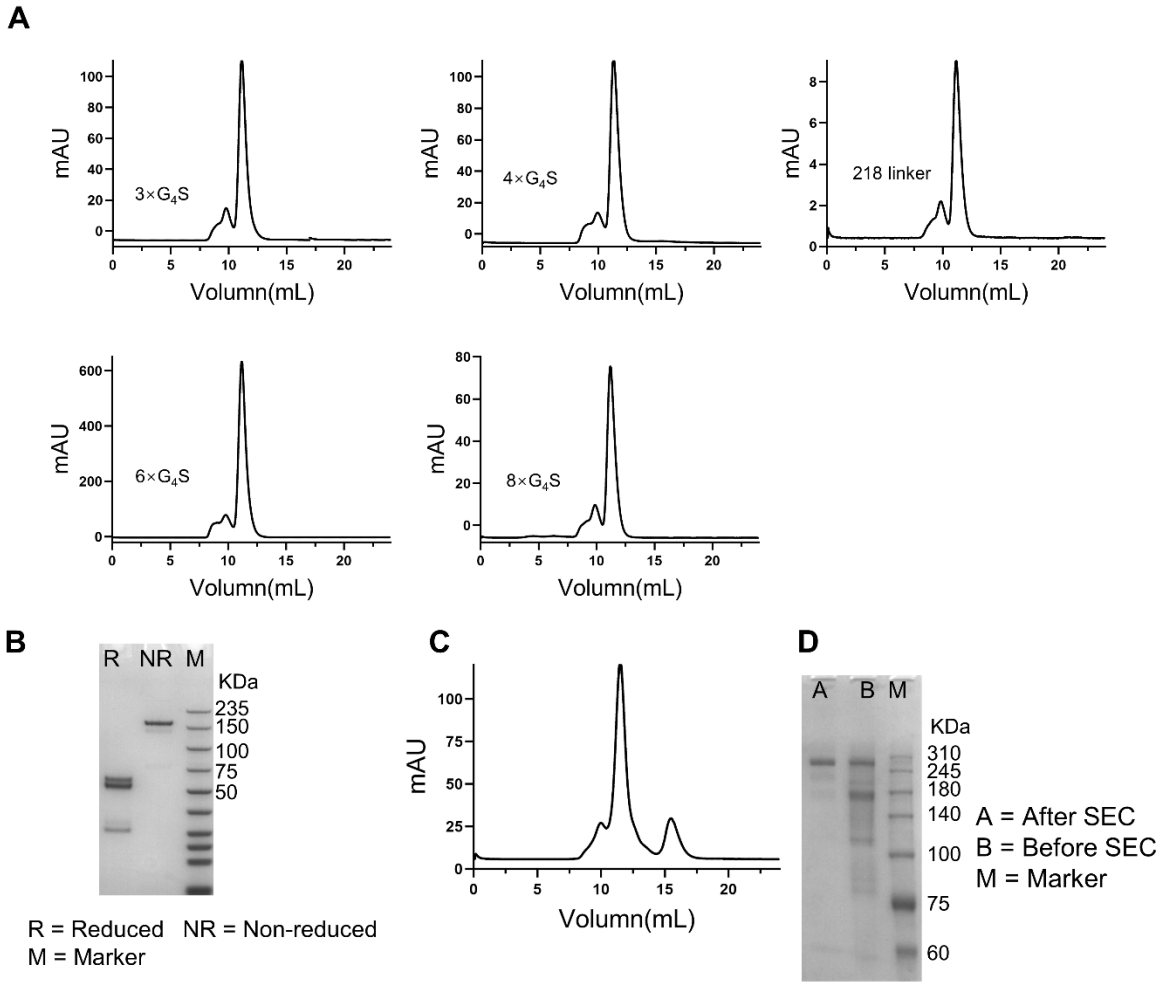


**Figure S1. Purification of X-bodies and square-body.**

A) Size-exclusion chromatography (SEC) results of X-bodies with different linkers (3×G4S, 4×G4S, 218 linker,6×G4S, and 8×G4S) between the light chain and the IgA Fc in the chimeric chain. B) Reducing and non-reducing SDS-PAGE results of anti-human CD20 X-body with 6×G4S linker. C) SEC result of anti-human CD20 square-body with 6×G4S linker. D) Non-reducing SDS-PAGE results of the square-body sample in (C).

A

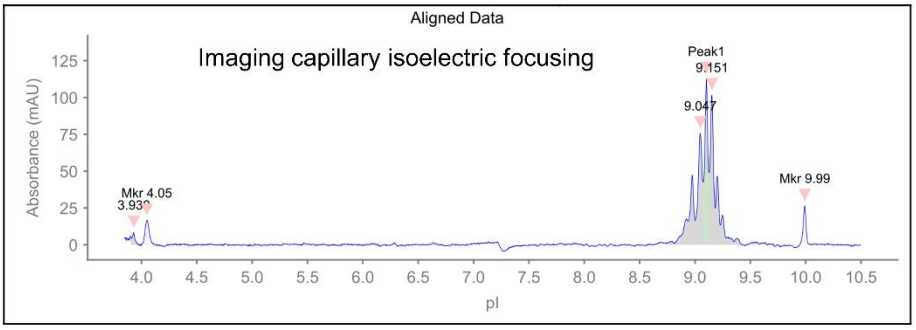


B

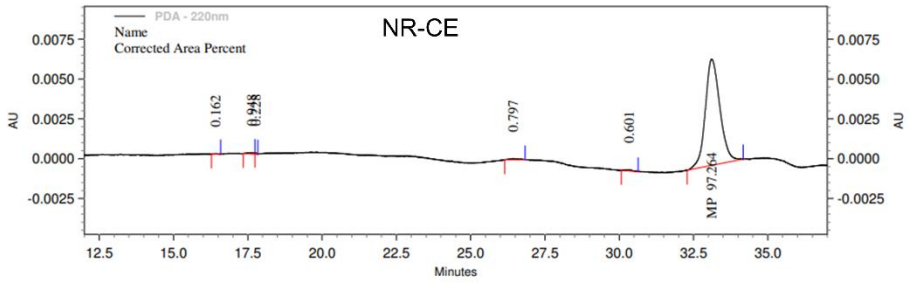


C

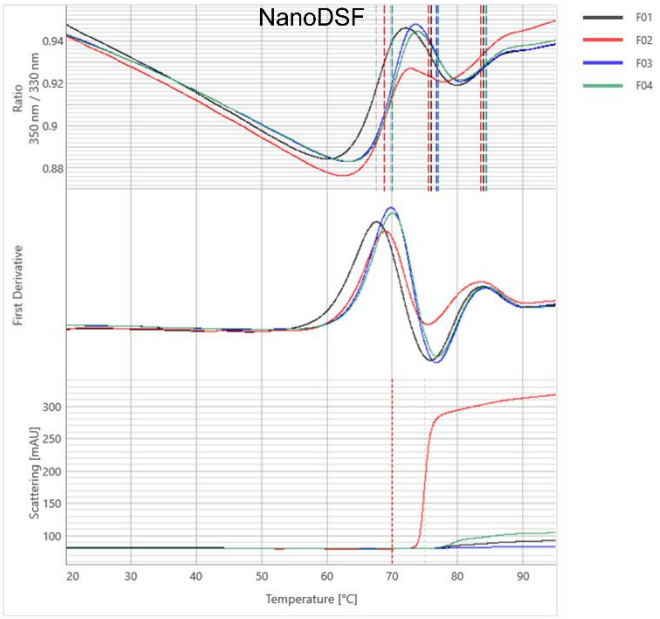


D

| | $T_m$ ℃ | $T_a$ ℃ | Particle size(nm) | Concentration(mg mL$^{-1}$) |
|---|---|---|---|---|
| **F01** | 75.9 | N/A | 13.8 | 6.0 |
| **F02** | 75.6 | 70.0 | 15.3 | 4.6 |
| **F03** | 76.9 | N/A | 14.2 | 5.8 |
| **F04** | 77.0 | 75.0 | 14.3 | 14.4 |

E

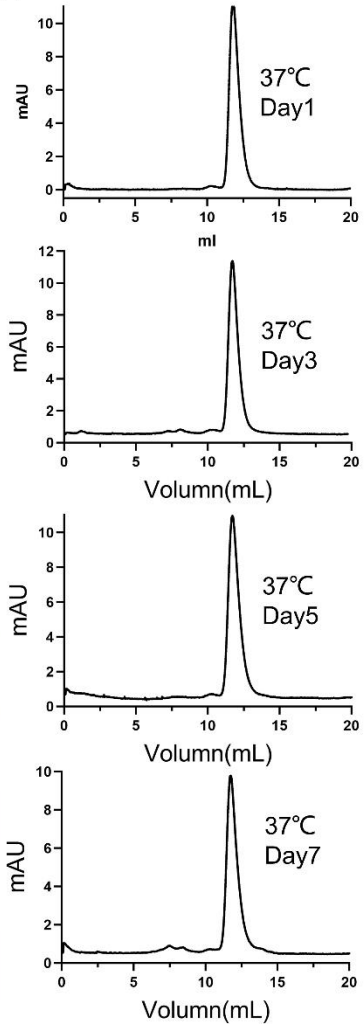

**Figure S2. characterization and stability assay of X-body.**

A) The pI analysis of the anti-hCD20 X-body (pI = 9.103) by imaging capillary isoelectric focusing (iCIE). B) The purity analysis of the anti-hCD20 X-body (97.3%) by non-reducing capillary electrophoresis (NR-CE). The detection wavelength was 220 nm and the sample was injected for 20 s. C) The $T_m$ of anti-hCD20 X-body in different buffers analyzed by the nano-format of Differential Scanning Fluorimetry (nanoDSF). F01 is PBS, F02 is HAC-NaAC buffer, F03 is CA-NaCA buffer and F04 is His-HCl buffer. D) The quantitative results of (C). E) The SEC profiles of X-body after 1, 3, 5 or 7 days of storage at 37°C.

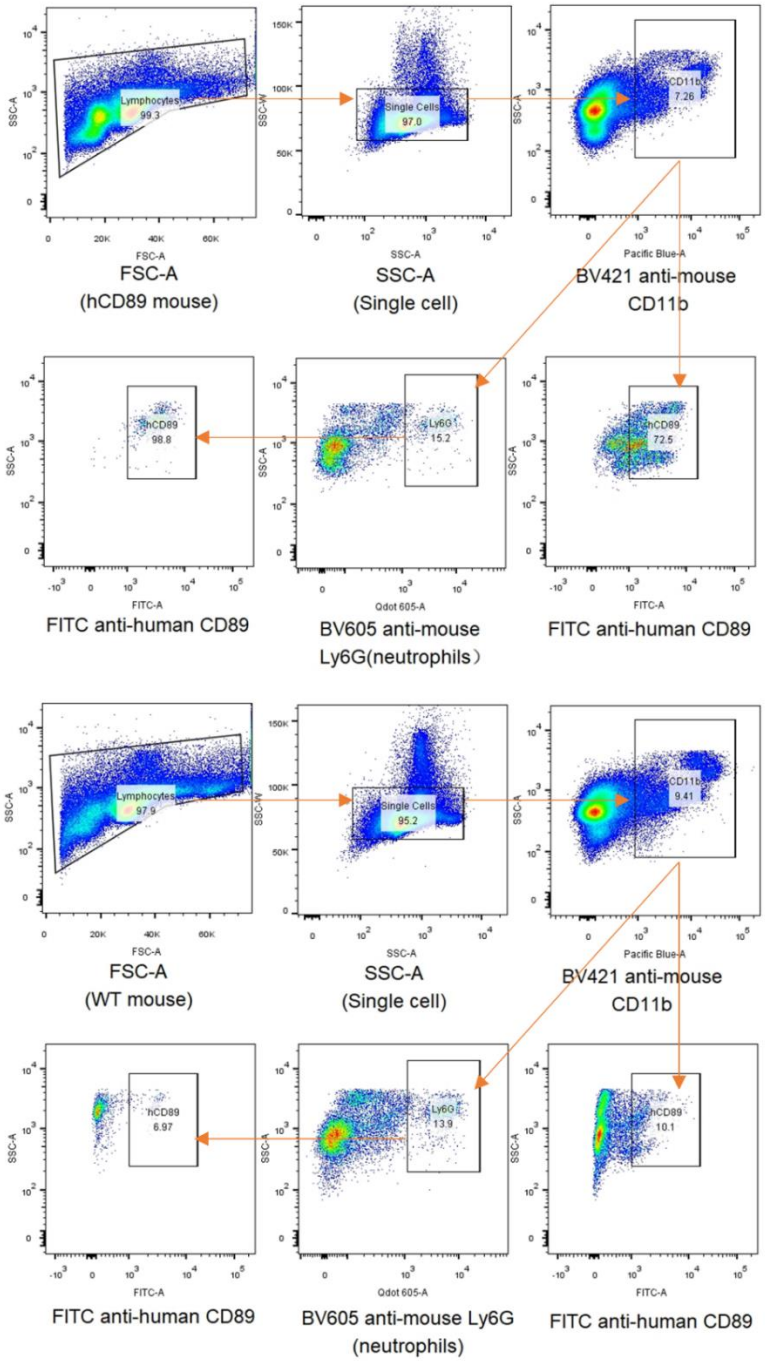


**Figure S3. Validation of the human CD89 transgenic C57BL/6J mice by flow cytometry.**

The figure depicts the gating strategies for identifying the expression of human CD89 in $CD11b^{+}$ cells and neutrophils from the spleen of human CD89 transgenic C57BL/6J mice or the wild-type mice.

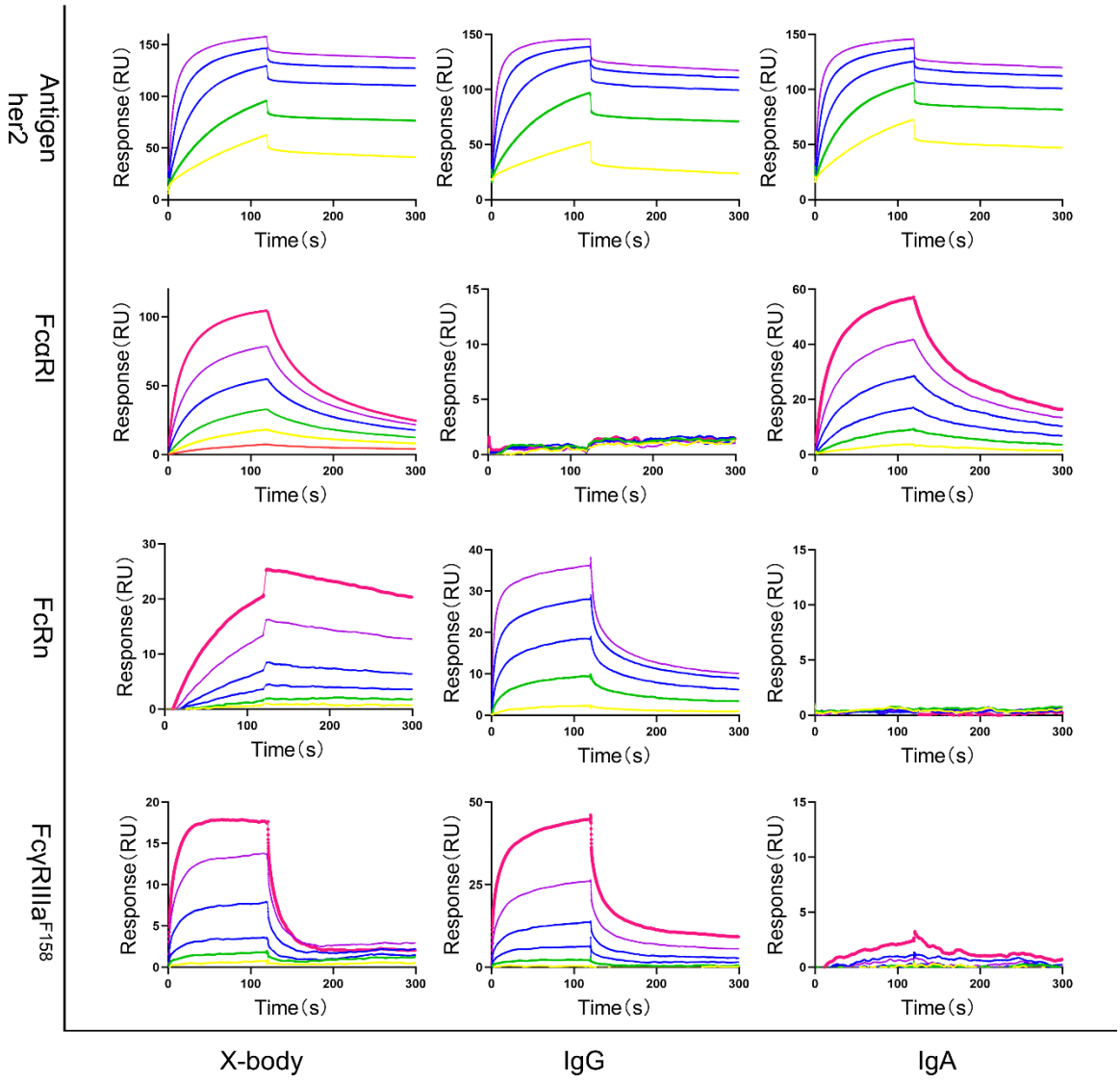


**Figure S4**. **Surface plasmon resonance analysis of trastuzumab antibodies binding to receptors and antigen (Her2).**

The binding of trastuzumab X-body to antigen HER2 and Fc receptors, such as CD89, FcRn and FcγRIIIa$^{F158}$, was evaluated by SPR. The IgA antibody used is monomeric IgA2 without the tailpiece for dimerization.

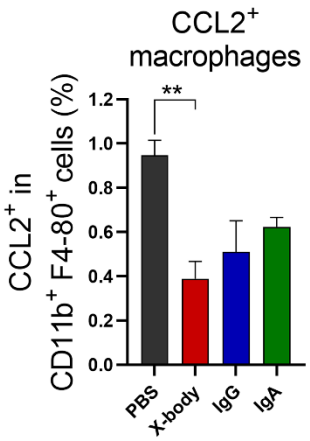


**Figure S5. The expression of the chemokine CCL2 of tumor associated macrophages in MC38-HER2 tumor cell bearing syngeneic model by using flow cytometry.**

MC38-HER2 cancer cells were subcutaneously implanted in human CD89 transgenic mice. When tumor reached 30-50 $mm^3$, the mice were treated with different version of trastuzumab. Tumor immune cells were isolated three days after 5 doses of drugs, stained with anti-CCL2 antibody and analyzed by flow cytometry. Data are presented as mean ± standard error of the mean (SEM). ** $p \leq 0.01$.

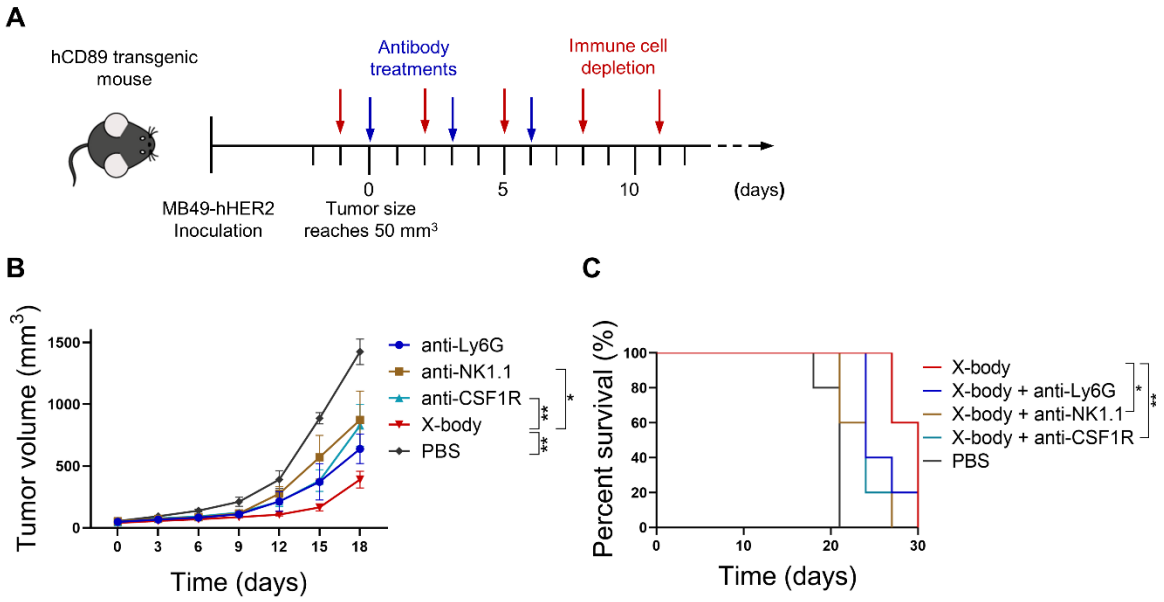


**Figure S6. NK cells, macrophages, and neutrophils are required to eliminate tumors in Her2 expressing MB49 model.**

A) Scheme of the treatment accompanied by immune cells depletion. MB49-HER2 cancer cells were subcutaneously implanted in human CD89 transgenic mice. Macrophages, neutrophils or NK cells were specifically depleted with anti-CSF1R, anti-Ly6G or anti-NK1.1 antibodies, respectively, prior to each dose of trastuzumab X-body. B) Tumor growth in the immune cell-depleted mice. C) Kaplan-Meier survival curves of the immune cell-depleted tumor-bearing mice. ** $p<0.01$, * $p<0.05$.

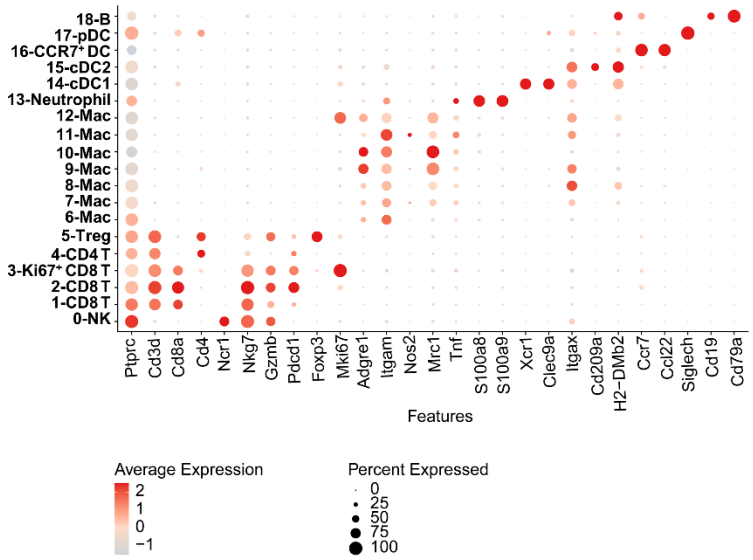


**Figure S7**. **Bubble heatmap showing marker genes across the 19 clusters from in Figure 6A.**

Dot size indicates the percent of expressing cells, and shades of color reflect normalized expression levels according to z-scores.

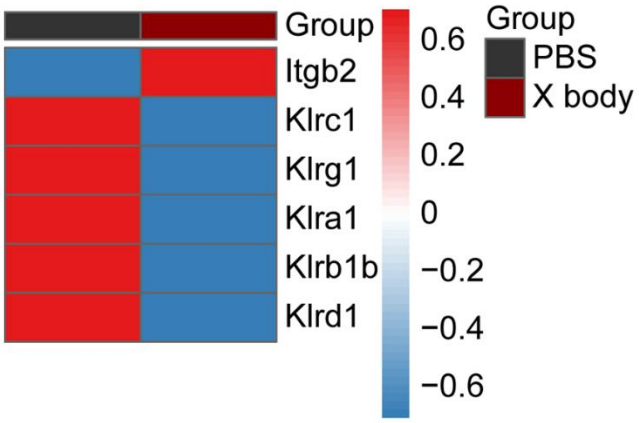


**Figure S8. Heatmap showing expression patterns of selected pathway genes for NK cells by scRNA-seq.**

Tumor infiltrating immune cells were isolated from mice in MB49-HER2 tumor models and subjected to single-cell RNA sequencing. Heatmap showed the inhibitory receptors of NK cells in PBS vehicle group (left) and X-body treatment group (right) by scRNA-seq.

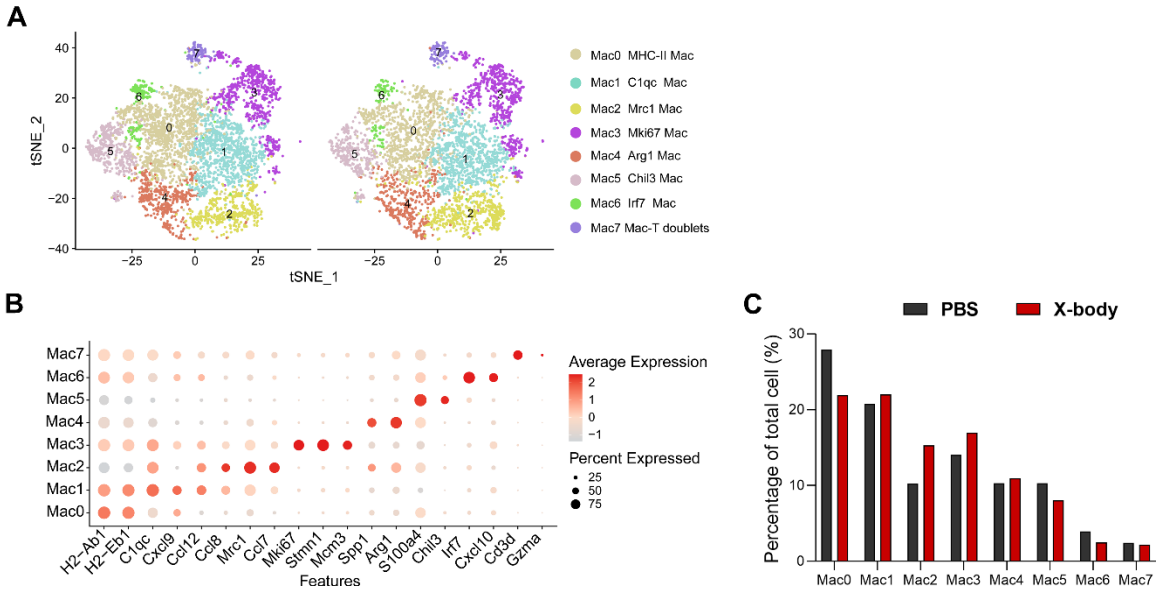


**Figure S9. Characterization of tumor-associated macrophages by scRNA-seq.**

A) t-SNE plot showing 8 subclusters of tumor-associated macrophages. B) Bubble heatmap showing marker genes across the 8 macrophage subclusters in (A). Dot size indicates the percent of expressing cells, and shades of color reflect normalized expression levels according to z-scores. C) Frequency of the 8 subclusters of tumor-associated macrophages.

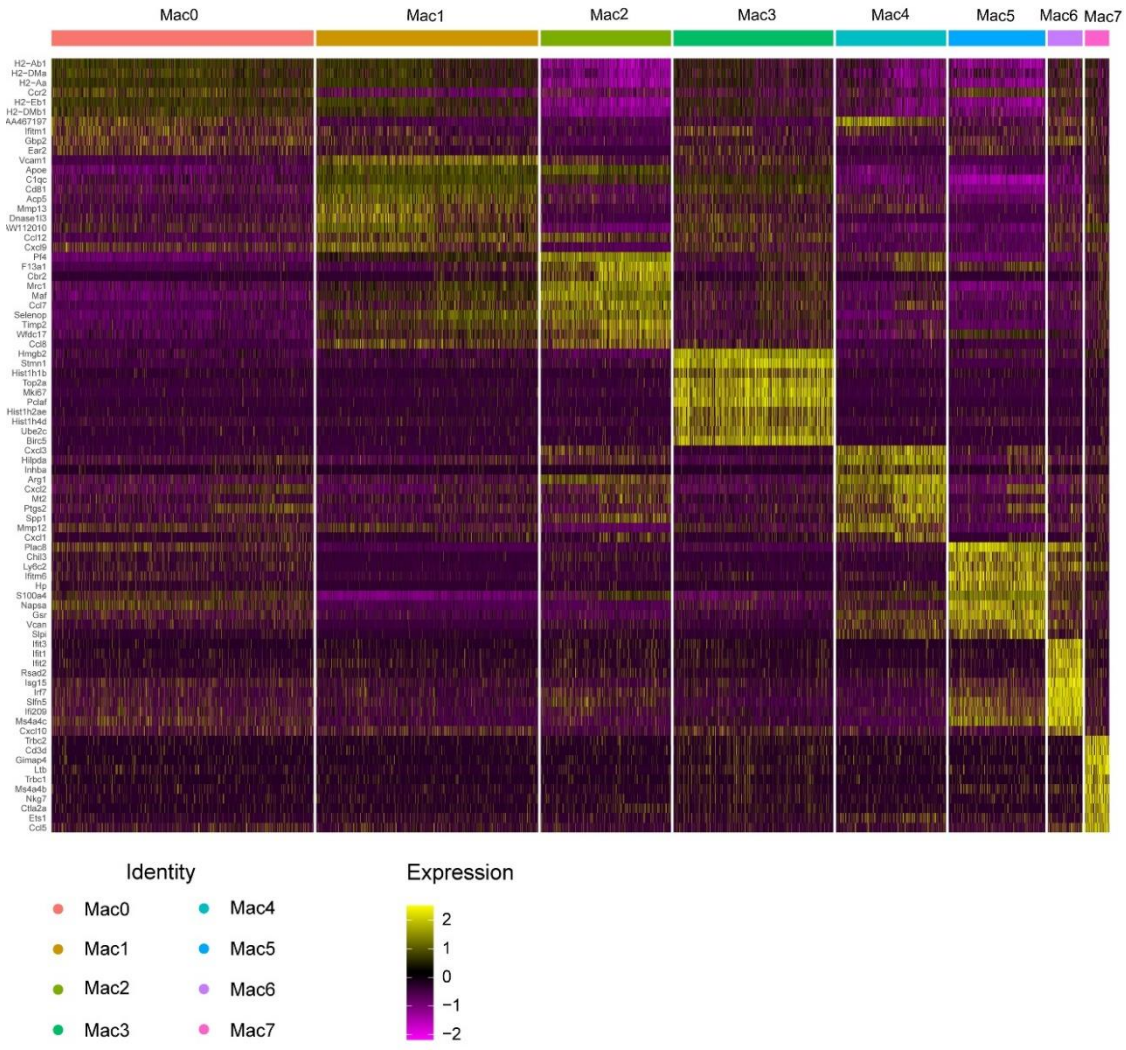


**Figure S10. Top ten gene expression heatmap of tumor-associated macrophages from MB49-HER2 tumor models by scRNA-seq.**

Tumor infiltrating immune cells were isolated from mice in MB49-HER2 tumor models and subjected to single-cell RNA sequencing. Heatmap showed the top ten gene expression levels of 8 subclusters of tumor-associated macrophages by scRNA-seq.

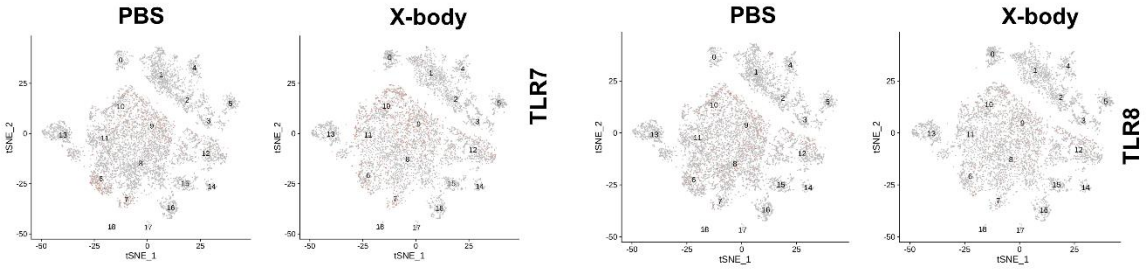


**Figure S11. Expression levels of genes such as TLR7 and TLR8 from mice bearing MB49-HER2 tumors by scRNA-seq.**

Tumor infiltrating immune cells were isolated from mice in MB49-HER2 tumor models and subjected to single-cell RNA sequencing. t-SNE plot showing expression levels of selected genes such as TLR7 and TLR8 of tumor-infiltrating immune cells in PBS vehicle group (left) and X-body treatment group (right) by scRNA-seq.

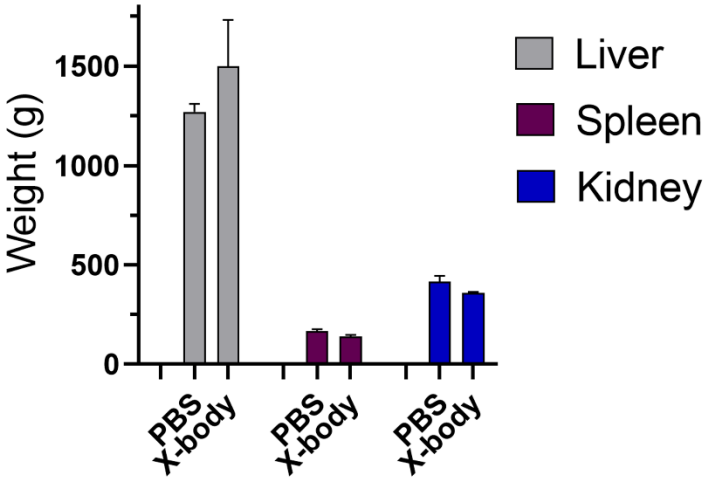


**Figure S12. The weights of liver, spleen and kidney from the mice treated with PBS or trastuzumab X-body.**

Human CD89 transgenic mice were treated with 10 mg/kg trastuzumab X-body or vehicle control. Liver, spleen and kidney were weighed.

**Table S1.** Amino acid sequences of Rituximab and Trastuzumab X-bodies.

| **Rituximab X-body** |
| --- |
| **Heavy chain:**<br><br>QVQLQQPGAELVKPGASVKMSCKASGYTFTSYNMHWVKQTPGRGLEWIGAIYPGNGDTSY<br>NQKFKGKATLTADKSSSTAYMQLSSLTSEDSAVYYCARSTYYGGDWYFNVWGAGTTVTVS<br>AASTKGPSVFPLAPSSKSTSGGTAALGCLVKDYFPEPVTVSWNSGALTSGVHTFPAVLQSSGL<br>YSLSSVVTVPSSSLGTQTYICNVNHKPSNTKVDKKVEPKSCDKTHTCPPCPAPELLGGPSVFLF<br>PPKPKDTLMISRTPEVTCVVVDVSHEDPEVKFNWYVDGVEVHNAKTKPREEQYNSTYRVVS<br>VLTVLHQDWLNGKEYKCKVSNKALPAPIEKTISKAKGQPREPQVYTLPPSRDELTKNQVSLT<br>CLVKGFYPSDIAVEWESNGQPENNYKTTPPVLDSDGSFFLYSKLTVDKSRWQQGNVFSCSVM<br>HEALHNHYTQKSLSLSPGK<br>**Chimeric chain:**<br><br>QIVLSQSPAILSASPGEKVTMTCRASSSVSYIHWFQQKPGSSPKPWIYATSNLASGVPVRFSGS<br>GSGTSYSLTISRVEAEDAATYYCQQWTSNPPTFGGGTKLEIKRTVAAPSVFIFPPSDEQLKSGT<br>ASVVCLLNNFYPREAKVQWKVDNALQSGNSQESVTEQDSKDSTYSLSSTLTLSKADYEKHK<br>VYACEVTHQGLSSPVTKSFNRGECGGGGSGGGGSGGGGSGGGGSGGGGSGGGGSVPPPPPC<br>CHPRLSLHRPALEDLLLGSEANLTCTLTGLRDASGATFTWTPSSGKSAVQGPPERDLCGCYSV<br>SSVLPGCAQPWNHGETFTCTAAHPELKTPLTANITKSGNTFRPEVHLLPPPSEELALNELVTLT<br>CLARGFSPKDVLVRWLQGSQELPREKYLTWASRQEPSQGTTTYAVTSILRVAAEDWKKGET<br>FSCMVGHEALPLAFTQKTIDRMAGK |
| **Trastuzumab X-body** |
| **Heavy chain:**<br><br>EVQLVESGGGLVQPGGSLRLSCAASGFNIKDTYIHWVRQAPGKGLEWVARIYPTNGYTRYA<br>DSVKGRFTISADTSKNTAYLQMNSLRAEDTAVYYCSRWGGDGFYAMDYWGQGTLVTVSSA<br>STKGPSVFPLAPSSKSTSGGTAALGCLVKDYFPEPVTVSWNSGALTSGVHTFPAVLQSSGLYS<br>LSSVVTVPSSSLGTQTYICNVNHKPSNTKVDKKVEPKSCDKTHTCPPCPAPELLGGPSVFLFPP<br>KPKDTLMISRTPEVTCVVVDVSHEDPEVKFNWYVDGVEVHNAKTKPREEQYNSTYRVVSVL<br>TVLHQDWLNGKEYKCKVSNKALPAPIEKTISKAKGQPREPQVYTLPPSRDELTKNQVSLTCL<br>VKGFYPSDIAVEWESNGQPENNYKTTPPVLDSDGSFFLYSKLTVDKSRWQQGNVFSCSVMH<br>EALHNHYTQKSLSLSPGK<br>**Chimeric chain:** |

DIQMTQSPSSLSASVGDRVTITCRASQDVNTAVAWYQQKPGKAPKLLIYSASFLYSGVPSRFS
GSRSGTDFTLTISSLQPEDFATYYCQQHYTTPPTFGQGTKVEIKRTVAAPSVFIFPPSDEQLKSG
TASVVCLLNNFYPREAKVQWKVDNALQSGNSQESVTEQDSKDSTYSLSSTLTLSKADYEKH
KVYACEVTHQGLSSPVTKSFNRGECGGGGSGGGGSGGGGSGGGGSGGGGSGGGGSVPPPPP
CCHPRLSLHRPALEDLLLGSEANLTCTLTGLRDASGATFTWTPSSGKSAVQGPPERDLCGCYS
VSSVLPGCAQPWNHGETFTCTAAHPELKTPLTANITKSGNTFRPEVHLLPPPSEELALNELVTL
TCLARGFSPKDVLVRWLQGSQELPREKYLTWASRQEPSQGTTTYAVTSILRVAAEDWKKGE
TFSCMVGHEALPLAFTQKTIDRMAGK

**Table S2.** The equilibrium constants of Rituximab antibodies.

| | $K_D$（nM) | | | | | | | |
|---|---|---|---|---|---|---|---|---|
| | **CD20** | **FcαRI** | **FcRn** | **FcγRI** | **FcγRIIa$^{H131}$** | **FcγRIIIA$^{F158}$** | **FcγRIIIA$^{V158}$** | **FcγRIIb** |
| **X-body** | 8.04 | 0.291 | 0.0613 | 0.0102 | 0.0364 | 0.0216 | 0.0240 | 0.00422 |
| **IgG** | 3.74 | ND | 0.0391 | 0.0115 | 0.0548 | 0.0663 | 0.0603 | 0.00277 |
| **IgA** | 6.71 | 0.314 | ND | 0.00324 | ND | ND | ND | ND |

ND: Not detectable